Efficient Solution of Many-objective Home Energy Management Systems

Marcos Tostado-Véliz[1], Samundra Gurung[2], Francisco Jurado[1,]*

[1]*Department of Electrical Engineering, University of Jaén, 23700 EPS Linares, Jaén, Spain*
[2]*Kathmandu University*

Abstract - Home Energy Management systems have become an essential tool on pursuing an efficient energy consumption besides the implantation of demand response programs in residential consumers. This kind of systems have evolved from a single-objective paradigm, in which only the electricity bill was concerned, to many-objective frameworks that involve different targets such as grid supporting programs or user convenience premises. From the computational point of view, many-objective optimization problems are more challenging than single-, and multiple-objective ones due to higher computational burden and the necessity of advanced tools capable to reach a compromise solution among objectives. This paper tackles this issue by developing an efficient but effective stochastic many-objective solution framework based on Mixed Integer Linear Programming formulation. The new proposal is based on lexicographic optimization and scalarizing functions, thus allowing to distinguish one of the targets as the most important one. This feature makes the new approach very suitable for Home Energy Management systems in which the energy cost is normally the most important objective while other goals can be considered secondary. The developed tool is validated on a standard home layout benchmark considering up to six typical objectives. The results obtained put on manifest the effectiveness and efficiency of the developed approach.

Keywords: Home Energy Management, Smart home, Multi-objective optimization, Many-objective optimization, Mixed Integer Linear Programming, Stochastic programming.

----

*Corresponding author, Tel.: +34 953 648518; Fax: +34 953 648586.
E-mail addresses: fjurado@ujaen.es (F. Jurado), mtostado@ujaen.es (M. Tostado-Véliz), samundra24@gmail.com (S. Gurun)

Nomenclature

Indexes (Sets)

$s(\mathcal{S})$	scenario
$r(\mathcal{R})$	representative scenario
$t(\mathcal{T})$	time
$k(\mathcal{K}^{\mathrm{NI}}/\mathcal{K}^{\mathrm{I}})$	uninterruptible/interruptible controllable appliance
Ω	cluster of a representative scenario
Ψ	time window $\Psi^k = [\mathrm{L}^k, \dots, \mathrm{U}^k];\ \forall k \in \mathcal{K}^{\mathrm{NI}} \cup \mathcal{K}^{\mathrm{I}}$

Functions

$\mathrm{avg}(\cdot)$	yields the mean value
$\mathrm{size}(\cdot)$	yields the number of elements within a cluster or set

Superscripts

Grid	utility grid
PV	photovoltaic
$\mathrm{BES, ch/dch}$	battery energy storage in charging/discharging mode
PEV	plug-in electric vehicle
$\mathrm{arr/dep}$	arrival/departure
$\mathrm{HVAC, h/c}$	heating-ventilation-air conditioner system in heating/cooling mode
EWH	electric water heater
$\mathrm{W, h/c}$	hot/cool water
$\mathrm{Air, in/out}$	indoor/outdoor air
$\mathrm{sp/db}$	set-point/dead-band
Build	building
Peak	peak
$\overline{(\cdot)}/\underline{(\cdot)}$	maximum/minimum value
$\widehat{(\cdot)}$	forecast value of an uncertain parameter
$\widetilde{(\cdot)}$	normalized value

Parameters

ω	probability (pu)
$\Delta\tau$	time step (hrs)
λ	energy cost (€/kWh)
d	non-controllable appliances demand (kW)
η	efficiency (pu)
ϑ	solar irradiation (kW/m²)
DOD	depth of discharge (pu)
δ	time slots of the operating cycle of a controllable appliance (-)
m	mass (kg)
C	heat or thermal capacity ($\mathrm{kJ}/(\mathrm{kg}\cdot{}^{\circ}\mathrm{C})$ or kWh/ºC)
R	equivalent thermal resistance (kW/ºC)
COP	coefficient of performance (pu)
v	volume (gallons)
R	equivalent thermal resistance (J/ºC or kWh/ºC)
M	large positive number (-)
q	lexicographic relaxing constraint parameter (pu)
w	weight factor (-)

Decision variables

p	power (kW)
ε	energy stored (kWh)
u	commitment status (binary)
on/off	it takes 1 if an asset is activated/deactivated at time t and 0 otherwise (binary)
θ	temperature (ºC)
v, y, z	dummy variables (hrs, binary or ºC)

1 - Introduction

With the emergence of the smart grid concept at early 21st century [1], electricity infrastructures have evolved towards cooperative networks in which all the agents act in a coordinated way on pursuing a more efficient energy and assets utilization [2-4]. The evolution of conventional electricity networks to smarter grids has been possible because the development of communication infrastructures and advanced metering technologies enable bidirectional information exchanging among the different agents such as consumers, generators or utility companies [5].

The deployment of advanced communication channels allow an active participation of end-users in the power system operation. To this end, energy companies launch demand-response (DR) programs, by which consumers are encouraged to voluntary modify their consumption patterns on pursuing a more efficient and clean use of generation sources, besides incentive inversions on onsite generators and storage systems [6]. Due to residential consumers suppose a large portion of the total electricity consumption [7], energy companies have devoted considerable efforts on developing DR programs among these users. In this regard, promotion of price-, incentive-, or decision variables-based DR strategies has evidenced their capability to achieve multiple goals such as peak-to-average ratio (PAR) reduction or renewable energy penetration [8-10]. Nevertheless, implantation of DR programs at residential level is not a simple task due to complex appliance loads and random consumption patterns [11]. In this context, Home

Energy Management (HEM) systems have become an essential tool for the successful development of DR schemes for residential consumers [12].

The most conventional HEM program carries out a day-ahead scheduling plan for the different controllable home appliances and assets, in order to reduce the electricity bill [7]. This single-objective vision has evolved in order to incorporate home users preferences such as thermal comfort or waiting time [13]. In this regard, many authors agree in further developing the HEM perspective to multi-objective paradigms. Such is the case of [14], in which besides to minimizing the electricity bill, thermal comfort, plug-in electric vehicle (PEV) charging requirements and appliances scheduling preferences are considered. Li and Tsai developed in [15] a HEM program by which the controllable appliances can be freely scheduled, but the users preferences are taken into account via cost functions. The HEM system proposed in [16] enables adjustable set-points of heating/cooling underfloor units to maximize the thermal comfort. Geng, et al. developed in [17] a HEM program based on the Internet of Things which maximizes the home inhabitants scheduling convenience. In the reference [18], the authors compared various heuristic algorithms for solving the HEM problem, taking the minimization of the electricity bill and waiting time as benchmark multi-objective function. Similarly, the thermal comfort is incorporated besides to the monetary cost in [19]. The article [20] presented Foresee™, a user-centric HEM system which optimizes the electricity bill, thermal comfort, gas emissions, user convenience and batteries degradation. The program developed in [21] considers the operation cost, DR fatigue and tenants scheduling satisfaction casted as a stochastic multi-objective Mixed Integer Linear Programming (MILP) problem. The HEM system proposed in [22] includes the dissatisfaction due to the modification of demand routines provoked by the application of DR programs. Hussain, et al. developed in [23] an eco-friendly HEM system which includes environmental indices in the objective function. The authors in [24] compares two strategies for HEM optimization based on genetic algorithms, by which the electricity bill and grid-dependence are jointly minimized. Javadi, et al. [25, 26] developed multi-objective self-scheduling HEM models for photovoltaic(PV)-battery energy storage (BES) domestic systems with incremental block rate tariffs and users scheduling convenience. In [27], a multi-objective HEM system for energy cost and users satisfaction is developed and solved by using an improved metaheuristic technique.

Other existing HEM systems consider the grid operator point of view in order to achieve an acceptable overall satisfaction level. Recent examples are the references [28] and [29]. The former proposes a HEM model which contemplates the possibility of DR programs focused on exploiting the onsite renewable generation of smart homes for grid support. Whereas the latter, includes a cost function to minimize the degradation of the coupling transformer device.

A main objective of DR programs is adapting the end-users load profile to be as flatten as possible [13]. This way, peak demands and fast ramps are avoided thus supposing a more economic and reliable operation of power grids. Utility companies may encourage the adoption of such premises in HEM systems by means of price-, incentive-, or decision variables-based programs. This topic has been widely covered in multiple related references. A typical index to measure the degree of flattening of a load profile is the PAR. Various HEM programs recently proposed (e.g. see [30]) include the PAR in the objective function besides the electricity bill, thermal comfort, etc. However, due to the nonlinearity of the PAR, these references used heuristic or metaheuristic solvers which do not ensure the reachability of the global optima and present a non-modularity structure [31]. To overcome these issues, some authors have explored alternative indexes to achieve a PAR reduction without including this index explicitly in the problem.

Sattarpour, et al. proposed in [32] a multi-objective HEM strategy with minimization of the so-called load profile deviation, which is a function that measures the difference between the power purchased from the grid and the mean daily energy consumption. The HEM program developed in [33] minimizes the peak demand instead of the PAR. The nonlinearity caused by the max function to determine the peak demand is linearized including s dummy variable and additional constraints. The authors in [34] developed a lineal function to determine the PAR, however, it assumes perfect knowledge on the appliances power consumption, which limits its usage.

As deduced from the literature review above, some advanced HEM paradigms have evolved towards many-objective optimization problems. This kind of problems typically involve more than three objective functions [35]. Usually, solving a many-objective optimization problem is a challenging task. This is due to besides to the challenges posed by multi-objective problems (e.g contradictory objective functions), the computational effort supposes a key issue because the quantity of objectives involved makes computationally demanding the calculation of the Pareto-front [36]. The simplest approach to manage with such problems consists on converting the multi-objective function to a convex weighted sum of the objective functions, this way, the problem can be treated as a conventional single-objective function problem. The weights of the objective function are set on the basis of user preferences, thus, that objective which is considered more important is distinguished by a high weight. This approach, although simple, presents various problems like difficulty to deal with objective of different units or resulting Pareto fronts with a low density of solutions [37]. In this regard, the authors in [33] proposed a solution based on the cooperative game theory approach. Nevertheless, this methodology assumes that all the objectives have the same importance. In addition, the solution of this problem may be complex and time-consuming due to nonlinearities introduced in the super-criterion process. More recently, the authors in [26] proposed to solve the multi-objective HEM system by using the epsilon-constraint technique. This methodology produces all possible Pareto-optimal solutions and let the decision maker choosing the most suitable one. However, this approach may be time consuming due to the calculation of the Pareto front, which makes it unsuitable for many-objective problems [36].

In many-objective HEM problems, some of the existing formulations may be unsuitable; for instance, those approaches which use a nonlinear model of the HEM program may be extraordinarily time consuming, due to this kind of formulations require to use specific solvers or including additional variables and constraints [38]. On the other hand, other techniques require to solve many times the HEM problem, which makes them appropriate for bi-objective frameworks but totally unaffordable for many-objective paradigms [39]. In addition, conventional multi-objective paradigms do not normally allow to give priority to some objective function with respect the others. Finally, the existing related literature has been focused on bi-, or three-objective approaches [40, 41], while many-objective problems with more than three objectives haven not been covered yet in HEM tools. This paper aims at circumventing these issues and filling these gaps, by developing a novel HEM program which aims at being suitable for many-objective problems. The new proposal exploits lexicographic optimization and scalarizing functions to solve a many-objective HEM program with six objective functions, in which the electricity bill is taken as the primary function to be optimized and other secondary objectives are minimized subjected to acceptable limits over the main objective. The proposed approach is validated on a benchmark smart home layout including different optimization objectives. Other salient contributions of this paper are:

- The optimization problem is formulated as a MILP, thus the global optima can be efficiently reached and the mathematical formulation presented here can be straightforward adapted to different problems and home layouts.
- Six different objective functions for HEM problems are developed, which take into account different perspectives like users convenience or equipment degradation.
- To manage with uncertainty nature of some parameters (e.g. solar irradiation or home demand), a modular scenario-based approach is proposed which can be easily adapted to incorporate any stochastic model. This proposal exploits clustering techniques to reduce the scenario space and keep the model computationally tractable.
- A case study is performed including six different objective functions, in which supposes the first attempt to many-objective paradigms in HEM tools.

In the rest of this paper, Section 2 overviews the home system under study. The mathematical formulation of the conventional HEM problem is outlined in Section 3. Section 4 presents secondary objective functions which are taken as benchmark. The proposed approach to manage with many-objective HEM problems is developed in Section 5. The uncertainty modelling approach considered in this paper is described in Section 6. Section 7 presents various numerical results. Finally, this paper is concluded with Section 8.

2 - Overview of the home system under study

This paper takes a standard home layout as benchmark [10, 25, 31], which is schematically depicted in Fig. 1. As seen, the home system can be supplied directly from the utility grid or through of onsite generators and storage assets. In this paper we consider the most typical solution in smart homes formed by PV panels and batteries [10, 25]. The domestic appliances are divided into two categories. On the one hand, the non-controllable appliances are managed on the basis of human decisions and cannot be controlled by the HEM system. On the other hand, the controllable appliances are scheduled by the HEM system within allowable time windows. The thermostatically controlled appliances (heating-ventilation-air conditioner (HVAC) system and electric water heater (EWH) in our case) are scheduled thus the room and hot water temperatures are kept within acceptable limits, respectively. The PEV may be charged from a unidirectional converter so that vehicle-to-home capabilities are not considered in this paper. Hereinafter, it is assumed that stochastic parameters such as ambient temperature or non-controllable appliances demand can be predicted with sufficiently day-ahead accuracy.

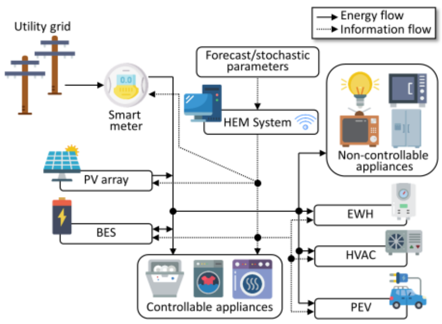

Fig. 1 Schematic representation of the home system under study

3 - Conventional HEM problem

This section describes the conventional HEM problem, by which the electricity bill is considered as the unique objective to be minimized [10, 31]. As this problem has been widely studied in the literature, this section only provides a brief description while the reader is referred to [10, 42] for further explanation.

It is worth noting that the problem described through this section is referred to the representative scenario space addressed by $\mathcal{R}$. This approach serves to uncertainty modelling (see Section 6).

3.1 - Home balance

In this paper it is assumed that unserved load is not allowed, so that the home demand must be fully supplied by either the local grid or onsite assets. This condition is ensured by imposing the constraint (1).

$$p_{r|t}^{\mathrm{Grid}} + p_{r|t}^{\mathrm{PV}} + p_{r|t}^{\mathrm{BES,dch}} = \hat{d}_{r|t} + p_{r|t}^{\mathrm{BES,ch}} + p_{r|t}^{\mathrm{PEV}} + \sum_{\forall k \in \mathcal{K}^{\mathrm{U}} \cup \mathcal{K}^{\mathrm{I}}} \left\{ u_{r|t}^{k} \cdot p^{k} \right\} + \sum_{\forall i \in \{\mathrm{h,c}\}} \left\{ p_{r|t}^{\mathrm{HVAC},i} \right\} + p_{r|t}^{\mathrm{EWH}};\ \forall r \in \mathcal{R}, t \in \mathcal{T} \quad (1)$$

3.2 - Grid modelling

In the simplest HEM problem, the utility grid can be modelled by an upper bound in the amount of energy that can be purchased from, which is imposed by contractual or technical limitations. This restriction is modelled by the constraint (2).

$$0 \le p_{r|t}^{\mathrm{Grid}} \le \bar{p}^{\mathrm{Grid}};\ \forall r \in \mathcal{R}, t \in \mathcal{T} \quad (2)$$

3.3 - PV array modelling

The amount of energy that can be generated for a set of PV panels is determined by the solar irradiation and ambient temperature. These parameters can be converted to units of power by using some component model formula, such as that used in [42] and casted in the equation (3).

$$\hat{p}_{r|t}^{\mathrm{PV}} = \overline{p}^{\mathrm{PV}} \cdot \left[0.25 \cdot \hat{\vartheta}_{r|t} + 0.03 \cdot \hat{\vartheta}_{r|t} \cdot \hat{\theta}_{r|t}^{\mathrm{air,out}} + (1.01 - 1.13 \cdot \eta^{PV}) \cdot \hat{\vartheta}_{r|t}^{2} \right];\ \forall r \in \mathcal{R}, t \in \mathcal{T} \quad (3)$$

As commented in [42], the expression (3) may yield a value higher than $\overline{p}^{\mathrm{PV}}$, which is not realistic since, in practise, solar inverters bound the power given by PV panels for security reasons and to avoid faster aging of equipment. Typically, this upper bound is fixed by 10% over the peak power of the PV unit, thus, the constraint (4) has to be imposed.

$$0 \le p_{r|t}^{\mathrm{PV}} \le \begin{cases} \hat{p}_{r|t}^{\mathrm{PV}}, & \text{if } \hat{p}_{r|t}^{\mathrm{PV}} \le 1.1 \cdot \overline{p}^{\mathrm{PV}} \\ \overline{p}^{\mathrm{PV}}, & \text{o.w.} \end{cases};\ \forall r \in \mathcal{R}, t \in \mathcal{T} \quad (4)$$

As seen above, the instantaneous power given by the PV array can be continuously controlled even below of $\hat{p}_{r|t}^{\mathrm{PV}}$. This is due to PV potential may be eventually not fully exploited during periods of low demand or fully charging of batteries. In such situation, surplus energy is dissipated in dummy loads. In this paper, explicit modelling of such loads is avoided since the constraint (4) actually reflects their impact.

3.5 - BES modelling

The equation (5) models the state of charge of the BES system as a function of the charging and discharging powers, which are limited to rated values, as said the constraint (6). Also, the charging and discharging processes of a BES unit are complementary [42], which is ensured by imposing the constraint (7). The constraint (8) bounds the amount of energy stored in batteries by the nominal capacity and the depth-of-discharge settings. The model described by (5)-(8) requires the initial and final state of charge of the battery bank to be fixed. In this paper, as customary [43, 44], it is assumed that the batteries are fully charged at the beginning and end of the time horizon, as said the constraint (9).

$$\varepsilon_{r|t}^{\mathrm{BES}} = \varepsilon_{r|t-1}^{\mathrm{BES}} + \Delta\tau \cdot \left(\eta^{\mathrm{BES}} \cdot p_{r|t}^{\mathrm{BES,ch}} - \frac{p_{r|t}^{\mathrm{BES,dch}}}{\eta^{\mathrm{BES}}}\right);\ \forall r \in \mathcal{R}, t \in \mathcal{T} \backslash t > 1 \quad (5)$$

$$0 \le p_{r|t}^{\mathrm{BES},i} \le u_{r|t}^{\mathrm{BES},i} \cdot \bar{p}^{\mathrm{BES}};\ \forall r \in \mathcal{R}, t \in \mathcal{T}, i \in \{\mathrm{ch}, \mathrm{dch}\} \quad (6)$$

$$0 \le \sum\nolimits_{\forall i \in \{\mathrm{ch,dch}\}} \left\{u_{r|t}^{\mathrm{BES},i}\right\} \le 1;\ \forall r \in \mathcal{R}, t \in \mathcal{T} \quad (7)$$

$$(1 - \mathrm{DOD}^{\mathrm{BES}}) \cdot \bar{\varepsilon}^{\mathrm{BES}} \le \varepsilon_{r|t}^{\mathrm{BES}} \le \bar{\varepsilon}^{\mathrm{BES}}; \forall r \in \mathcal{R}, t \in \mathcal{T} \quad (8)$$

$$\varepsilon_{r|1}^{\mathrm{BES}} = \varepsilon_{r|\,\mathrm{size}(\mathcal{T})}^{\mathrm{BES}} = \bar{\varepsilon}^{\mathrm{BES}};\ \forall r \in \mathcal{R} \quad (9)$$

3.6 - PEV modelling

As commented, in this paper is considered the vehicle-to-home capability of the PEV cannot be exploited due to expensive expenditures dedicated to bi-directional chargers are not always justified. In this sense, the PEV is modelled similar to the battery bank. Hence, the equation (10) models the state of charge of the PEV as a function of the charging power, which is limited to its nominal value, as said the constraint (11). As in the case of the battery bank, the amount of energy stored in the onsite batteries is limited by their nominal capacity and the depth-of-discharge settings by the constraint (12).

$$\varepsilon_{r|t}^{\mathrm{PEV}} = \varepsilon_{r|t-1}^{\mathrm{PEV}} + \Delta\tau \cdot \eta^{\mathrm{PEV}} \cdot p_{r|t}^{\mathrm{PEV}};\ \forall r \in \mathcal{R}, t \in \mathcal{T} \backslash t > 1 \tag{10}$$
$$0 \leq p_{r|t}^{\mathrm{PEV}} \leq \bar{p}^{\mathrm{PEV}};\ \forall r \in \mathcal{R}, t \in \mathcal{T} \tag{11}$$
$$(1 - \mathrm{DOD}^{\mathrm{PEV}}) \cdot \bar{\varepsilon}^{\mathrm{PEV}} \leq \varepsilon_{r|t}^{\mathrm{PEV}} \leq \bar{\varepsilon}^{\mathrm{PEV}}; \forall r \in \mathcal{R}, t \in \mathcal{T} \tag{12}$$

For simplicity, it is assumed that the PEV arrives at the beginning of the time horizon. The state of charge at this time slot is unknown as this parameter depends on the daily mileage [45]. Therefore, it is treated as an uncertain parameter (see Section 6). Typically, home users desire to get the PEV fully charged at its departure time, which is ensured by the constraint (13). Intuitively, the PEV cannot be charged during those hours in which it is not parked at home, which is modelled with (14).

$$\varepsilon_{r|t^{\mathrm{PEV,dep}}}^{\mathrm{PEV}} = \bar{\varepsilon}^{\mathrm{PEV}};\ \forall r \in \mathcal{R} \tag{13}$$
$$\sum_{\forall t \notin \{t^{\mathrm{PEV,arr}} : t^{\mathrm{PEV,dep}}\}} \left\{p_{r|t}^{\mathrm{PEV}}\right\} = 0; \forall r \in \mathcal{R} \tag{14}$$

3.7 - Controllable appliances modelling

Controllable appliances are broadly classified into non-interruptible and interruptible [13]. For the first class, the operating cycle cannot be interrupted once it has started. Contrarily, the operating cycle of an interruptible appliance can be interrupted for convenience. In any case, the controllable appliances must complete their duty cycles within allowable time windows. Under these considerations, the controllable appliances are modelled by the set of constraints (15)-(17).

$$\sum_{\forall t \in \Psi^k} \left\{u_{r|t}^{k}\right\} = \delta^k;\ \forall r \in \mathcal{R}, k \in \mathcal{K}^{\mathrm{NI}} \cup \mathcal{K}^{\mathrm{I}} \tag{15}$$
$$\sum_{\forall t \in T} \left\{\mathrm{on}_{r|t}^{k}\right\} = 1;\ \forall r \in \mathcal{R}, k \in \mathcal{K}^{\mathrm{NI}} \cup \mathcal{K}^{\mathrm{I}} \tag{16}$$
$$u_{r,t}^{k} - u_{r,t-1}^{k} = \mathrm{on}_{r,t}^{k} - \mathrm{off}_{r,t}^{k};\ \forall r \in \mathcal{R}, t \in \mathcal{T} \backslash t > 1, k \in \mathcal{K}^{\mathrm{NI}} \tag{17}$$

3.8 - Thermostatically controlled appliances modelling

The home system depicted in Fig. 1 includes a HVAC system and a EWH, which are devoted on keeping the room and hot water temperatures within acceptable limits. In this paper we adopt a linear model for the indoor temperature [31, 46], as stated the equations (18)-(20).

$$\theta_{r|t}^{\text{Air,in}} = \left(1 - \frac{\Delta\tau}{10^3 \cdot m^{\text{Air,in}} \cdot C^{\text{Air,in}} \cdot R^{\text{Build}}}\right) \cdot \theta_{r|t-1}^{\text{Air,in}} + \frac{1}{10^3 \cdot m^{\text{Air,in}} \cdot C^{\text{Air,in}} \cdot R^{\text{Build}}} \cdot \theta_{r|t-1}^{\text{Air,out}} + \frac{\left(p_{r|t-1}^{\text{HVAC,h}} - p_{r|t-1}^{\text{HVAC,c}}\right)}{0.000277 \cdot m^{\text{Air,in}} \cdot C^{\text{Air,in}}} \cdot \text{COP}^{\text{HVAC}};\ \forall r \in \mathcal{R}, t \in \mathcal{T} \backslash t > 1 \tag{18}$$

$$\theta_{r|t+1}^{\text{W,h}} = \theta_{r|t}^{\text{Air,in}} + p_{r|t}^{\text{EWH}} \cdot \eta^{\text{EWH}} \cdot C^{\text{W,h}} - \left(\theta_{r|t}^{\text{Air,in}} - \theta_{r|t}^{\text{W,h}}\right) \cdot e^{\left(\frac{-\Delta\tau}{R^{\text{W,h}} \cdot C^{\text{W,h}}}\right)};\ \forall r \in \mathcal{R}, t \in \mathcal{T} \backslash t < \text{size}(\mathcal{T}), v_{s|t}^{\text{W,h}} = 0 \tag{19}$$

$$\theta_{r|t+1}^{\text{W,h}} = \frac{\theta_{r|t}^{\text{W,h}} \cdot \left(\overline{v}^{\text{EWH}} - v_{r|t}^{\text{W,h}}\right) + \theta_{r|t}^{\text{W,c}} \cdot v_{r|t}^{\text{W,h}}}{\overline{v}^{\text{EWH}}};\ \forall r \in \mathcal{R}, \forall t \in \mathcal{T} \backslash t < \text{size}(\mathcal{T}), v_{r|t}^{\text{W,h}} > 0 \tag{20}$$

Power consumption of thermostatically controlled appliances is upper bounded by nominal values, as ensured the constraints (21) and (22). In the case of the HVAC system, the constraint (23) is necessary to make the heating and cooling modes complementary processes.

$$0 \le p_{r|t}^{\text{HVAC},j} \le u_{r|t}^{\text{HVAC},i} \cdot \overline{p}^{\text{HVAC}};\ \forall r \in \mathcal{R}, t \in \mathcal{T}, i \in \{\text{h}, \text{c}\} \tag{21}$$

$$0 \le p_{r|t}^{\text{EWH}} \le \overline{p}^{\text{EWH}};\ \forall r \in \mathcal{R}, \forall t \in \mathcal{T} \tag{22}$$

$$\sum_{\forall i \in \{\text{h,c}\}} \left\{u_{r|t}^{\text{HVAC},i}\right\} \le 1;\ \forall r \in \mathcal{R}, t \in \mathcal{T} \tag{23}$$

As commented, the thermostatically controlled appliances are operated so that the indoor and hot water temperatures are kept within acceptable limits ensuring thermal comfort. In the case of the room temperature, dead-band terms are included in order to avoid a frequent operation of the HVAC system [46], as said the constraint (24). On the other hand, the hot water temperature has to be kept between the specified set-point and an upper bound which is imposed by security reasons [31], as forced by the constraint (25).

$$\theta^{\text{HVAC,sp}} - \theta^{\text{HVAC,db}} \le \theta_{r|t}^{\text{Air,in}} \le \theta^{\text{HVAC,sp}} + \theta^{\text{HVAC,db}};\ \forall r \in \mathcal{R}, t \in \mathcal{T} \tag{24}$$

$$\theta^{\text{W,h,sp}} \le \theta_{r|t}^{\text{W,h}} \le \overline{\theta}^{\text{W,h}};\ \forall r \in \mathcal{R}, \forall t \in \mathcal{T} \tag{25}$$

Similar to the BES model, the initial and final indoor and hot water temperatures have to be fixed. In our case, it is assumed that both are equal to their respective set-points as modelled by the equations (26) and (27).

$$\theta_{r|1}^{\text{Air,in}} = \theta_{r|\text{size}(\mathcal{T})}^{\text{Air,in}} = \theta^{\text{HVAC,sp}};\ \forall r \in \mathcal{R} \tag{26}$$

$$\theta_{s|1}^{\text{W,h}} = \theta_{s|\text{size}(\mathcal{T})}^{\text{W,h}} = \theta^{\text{W,h,sp}};\ \forall r \in \mathcal{R} \tag{27}$$

3.9 - Objective function

In the conventional HEM program, the minimization of the electricity bill is the most typical objective function. Therefore, the conventional HEM optimization problem is defined as follows

<u>Conventional HEM problem:</u>

$$\begin{aligned} &\min_{\Phi} f_1 = \textstyle\sum_{\forall r\in\mathcal{R}}\left\{\omega_r \cdot \sum_{\forall t\in\mathcal{T}}\left\{\Delta\tau \cdot \lambda_t \cdot p_{r|t}^{\text{Grid}}\right\}\right\} \\ &\text{s.t.}\,(1)-(27) \end{aligned} \tag{28}$$

where Φ is the vector of decision variables given by

$$\Phi = \begin{Bmatrix} p_{r|t}^{i}, p_{r|t}^{\text{BES},ii}, p_{r|t}^{\text{HVAC},iii}, \varepsilon_{r|t}^{iiii}, u_{r|t}^{\text{BES},ii}, \\ u_{r|t}^{\text{HVAC},iii}, u_{r|t}^{k}, \text{on}_{r|t}^{kk}, \text{off}_{r|t}^{kk} \end{Bmatrix};\ \forall r \in \mathcal{R}, t \in \mathcal{T}, k \in \mathcal{K}^{\text{NI}} \cup \mathcal{K}^{\text{I}}, kk \in \mathcal{K}^{\text{NI}}, i \in \{\text{Grid}, \text{PV}, \text{PEV}, \text{EWH}\}, ii \in \{\text{ch}, \text{dch}\}, iii \in \{\text{h}, \text{c}\}, iiii \in \{\text{BES}, \text{PEV}\} \tag{29}$$

4 - Alternative HEM objectives

Besides the minimization of the electricity bill, the most advanced HEM programs incorporated other secondary objectives devoted on maximizing the users thermal comfort or minimizing the waiting time, PAR or equipment degradation. Since this paper is focused on many-objective problems (which usually involves more than three objectives [35]), we develop up to five alternative objective functions which are devoted on improving different indicators. Subsequent sections present some of the most typical alternative objective functions in HEM programs.

4.1 - PAR reduction

Utility companies desire load profiles as flatten as possible [31]. This way, a more economical system operation is achieved since expensive fast ramping units are barely operated. The degree of flattening of a load profile over the $\mathcal{R}$-space is given by

$$\mathrm{PAR} = \sum_{\forall r \in \mathcal{R}} \left\{ \omega_r \cdot \frac{\max_{\forall t \in \mathcal{T}} \left(p_{r|t}^{\mathrm{Grid}} \right)}{\operatorname{avg}_{\forall t \in \mathcal{T}} \left(p_{r|t}^{\mathrm{Grid}} \right)} \right\} \tag{30}$$

One can check that the function (31) has a global minimum equal to 1, for which the load profile is perfectly flat. Utility companies can encourage end-users to incorporate the PAR reduction in their HEM programs through incentive programs [8]. The PAR function cannot be directly managed in MILP problems because the nonlinearity brought by the division of variables. To overcome this issue, the reference [30] proposed the following equivalent function

$$\mathrm{PAR} = \sum_{\forall r \in \mathcal{R}} \left\{ \omega_r \cdot \left(\max_{\forall t \in \mathcal{T}} \left(p_{r|t}^{\mathrm{Grid}} \right) - \operatorname{avg}_{\forall t \in \mathcal{T}} \left(p_{r|t}^{\mathrm{Grid}} \right) \right) \right\} \tag{31}$$

Both (30) and (31) achieve their global minimum at the same point, however, in the case of (31), this minimum is equal to 0. The function (31) is still nonlinear because the nonlinearity of the max function. To manage with this nonlinear function and keep the model linear, we propose to linearize the max function by introducing the variable p_r^{Peak}, which is equal to the peak power if the constraint (32) is imposed.

$$p_r^{\mathrm{Peak}} \geq p_{r|t}^{\mathrm{Grid}};\ \forall r \in \mathcal{R}, t \in \mathcal{T} \tag{32}$$

Indeed, one can clearly check that p_r^{Peak} is forced to be equal to the peak power since this variable is minimized in the objective function. When the HEM program aims at minimizing the PAR, the constraint (33) is necessary since the controllable appliances could be scheduled out of their time windows in order to flat the demand curve as much as possible, which is not a realistic assumption.

$$\sum_{\forall t \notin \Psi^k} \left\{ u_{r|t}^k \right\} = 0;\ \forall r \in \mathcal{R}, k \in \mathcal{K}^{\mathrm{NI}} \cup \mathcal{K}^{\mathrm{I}} \tag{33}$$

With the model (31)-(33) the PAR can be introduced in the objective function and the MILP essence of the formulation is preserved. Thereby, the problem (34) defines a single-objective HEM program for PAR minimization.

<u>PAR reduction for HEM programs:</u>

$$\min_{\Phi, p_r^{\text{Peak}};\, \forall r \in \mathcal{R}} f_2 = \sum_{\forall r \in \mathcal{R}} \left\{ \omega_r \cdot \left(p_r^{\text{Peak}} - \operatorname*{avg}_{\forall t \in \mathcal{T}} \left(p_{r|t}^{\text{Grid}} \right) \right) \right\} \tag{34}$$
$$\text{s.t.}\ (1) - (27), (32), (33)$$

4.2 - Maximization of the thermal comfort

Other usual HEM objective is the maximization of the thermal comfort. Typically, this objective is devoted on keeping the room temperature as close as possible to the desired set-point over the studied time horizon. Therefore, the maximization of the thermal comfort is equivalent to the minimization of the difference between the instantaneous room temperature and the HVAC set-point. Mathematically, this problem is defined by (35).

<u>Maximization of the thermal comfort:</u>

$$\min_{\Phi, y_{r|t}, z_{r|t};\, \forall r \in \mathcal{R}, t \in \mathcal{T}} f_3 = \sum_{\forall r \in \mathcal{R}} \left\{ \omega_r \cdot \sum_{\forall t \in \mathcal{T}} \left\{ \underbrace{\left| \theta^{\text{HVAC,sp}} - \theta_{r|t}^{\text{Air,in}} \right|}_{z_{r|t}} \right\} \right\} \tag{35}$$
$$\text{s.t.}\ (1) - (27), (36) - (42)$$

The absolute value included in (35) makes this objective function nonlinear. To solve this issue, the absolute term in (35) can be replaced by the dummy variable z and the MILP structure of the problem is preserved by defining the dummy variable y and imposing the following set of constraints.

$$M \cdot y_{r|t} \geq \theta^{\text{HVAC,sp}} - \theta_{r|t}^{\text{Air,in}};\ \forall r \in \mathcal{R}, t \in \mathcal{T} \tag{36}$$
$$M \cdot \left(1 - y_{r|t}\right) \geq \theta_{r|t}^{\text{Air,in}} - \theta^{\text{HVAC,sp}};\ \forall r \in \mathcal{R}, t \in \mathcal{T} \tag{37}$$
$$z_{r|t} \geq \theta^{\text{HVAC,sp}} - \theta_{r|t}^{\text{Air,in}};\ \forall r \in \mathcal{R}, t \in \mathcal{T} \tag{38}$$
$$z_{r|t} \geq \theta_{r|t}^{\text{Air,in}} - \theta^{\text{HVAC,sp}};\ \forall r \in \mathcal{R}, t \in \mathcal{T} \tag{39}$$
$$z_{r|t} \leq \theta^{\text{HVAC,sp}} - \theta_{r|t}^{\text{Air,in}} + \theta^{\text{HVAC,db}} \cdot \left(1 - y_{r|t}\right);\ \forall r \in \mathcal{R}, t \in \mathcal{T} \tag{40}$$
$$z_{r|t} \leq \theta_{r|t}^{\text{Air,in}} - \theta^{\text{HVAC,sp}} + \theta^{\text{HVAC,db}} \cdot y_{r|t};\ \forall r \in \mathcal{R}, t \in \mathcal{T} \tag{41}$$
$$0 \leq z_{r|t} \leq \theta^{\text{HVAC,db}};\ \forall r \in \mathcal{R}, t \in \mathcal{T} \tag{42}$$

4.3 - Minimization of the waiting time of non-interruptible appliances

The scheduling inconvenience of home users is frequently involved in HEM programs. Assuming that tenants desire the controllable appliances be scheduled as soon as possible (i.e. start its operating cycle at $t = L$), the minimization of the waiting time referred to the non-interruptible appliances is addressed by the optimization problem (43).

Minimization of the waiting time (non-interruptible appliances):

$$\begin{aligned}&\min_{\Phi} f_4 = \textstyle\sum_{\forall r\in\mathcal{R}}\left\{\omega_r \cdot \left(\sum_{\forall k\in\mathcal{K}^{\mathrm{NI}}}\left\{\Delta\tau \cdot \left(\mathrm{on}_{r|t}^{k} \cdot \boldsymbol{\tau} - \mathrm{L}^{k}\right)\right\}\right)\right\}\\ &\text{s.t.}\,(1) - (27)\end{aligned} \quad (43)$$

where $\boldsymbol{\tau} = [1,2, \dots, \mathrm{size}(\mathcal{T})]^T$.

4.4 - Minimization of the waiting time of interruptible appliances

The objective (43) is not applicable in the case of interruptible appliances since this devices may present various on/off cycles during the scheduling horizon. To properly quantify the waiting time of these appliances, let us introduce the dummy variable v. This variable is equal to the last time slot in which an interruptible appliance is scheduled, in other words, this variable reflects the time instant in which an interruptible appliance completes its duty cycle. Therefore, the limits of v are imposed by the constraint (44).

$$1 \leq v_r^k \leq \mathrm{size}(\mathcal{T});\ \forall r \in \mathcal{R}, k \in \mathcal{K}^{\mathrm{I}} \quad (44)$$

To keep the coherency of the variable v, the following constraint is necessary.

$$v_r^k \geq u_{r|t}^k \cdot \boldsymbol{\tau}_t;\ \forall r \in \mathcal{R}, t \in \mathcal{T}, k \in \mathcal{K}^{\mathrm{I}} \quad (45)$$

Indeed, one can easily check that by (45) the variable v is forced to be equal to the last time slot in which an interruptible appliance is scheduled. Thus, by (15) and (45) this variable is equal to the time slot in which an interruptible appliance completes its duty cycle, as desired. This way, the minimization of the waiting time for the interruptible appliances is formulated by the problem (46).

Minimization of the waiting time (interruptible appliances):

$$\begin{aligned}&\min_{\Phi, v_r^k;\ \forall r\in\mathcal{R}, k\in\mathcal{K}^{\mathrm{I}}} f_5 = \textstyle\sum_{\forall r\in\mathcal{R}}\{\omega_r \cdot (\sum_{\forall k\in\mathcal{K}^{\mathrm{I}}}\{\Delta\tau \cdot (v_r^k - \mathrm{U}^k - \delta^k + 1)\})\}\\ &\text{s.t.}\,(1) - (27), (44), (45)\end{aligned} \quad (46)$$

4.5 - Minimization of the BES system degradation

The lifecycle of a BES system depends on multiple factors like the battery technology or the depth-of-discharge settings [44]. As these aspects are assumed to be preset and cannot be varied by the HEM tool, the battery aging is mainly determined by the total number of charging-discharging cycles completed over the studied time horizon. This aspect can be controlled by the HEM program insofar as the scheduling plan of the BES system is optimized. Thus, by using [44, eq. (26)] which defines the total number of charging-discharging completed through a year, the minimization of the BES aging can be formulated for the HEM problem by (47).

Minimization of the BES degradation:

$$\min_{\Phi} f_6 = \sum_{\forall r \in \mathcal{R}} \left\{ \frac{\omega_r \cdot \Delta\tau}{2 \cdot \bar{\varepsilon}^{\mathrm{BES}}} \cdot \sum_{\forall t \in \mathcal{T}} \left\{ p_{r|t}^{\mathrm{BES,ch}} + p_{r|t}^{\mathrm{BES,dch}} \right\} \right\} \quad \text{s.t. } (1) - (27) \tag{47}$$

5 - Proposed approach for many-objective HEM optimization

This paper is devoted on the solution of the many-objective HEM problem comprising the objective functions $f_1 - f_6$ described above. These objectives are contradictory, for instance, the thermal comfort cannot be maximized if the electricity bill is not increased as counterpart. On the other hand, home users typically give more importance to the monetary savings, thereby, they may be unwilling to enhance the thermal comfort or the PAR if it supposes a notably increment of the bill. Hence, the solution of the proposed many-objective HEM problem is not trivial.

Many approaches have been developed for multi-objective optimization problems. Most of them are devoted on calculating all the solutions on the so-called Pareto front. Formally, the Pareto front is defined as the set of solutions by which an objective cannot be enhanced without deteriorating others [35-37]. Calculation of the Pareto front may be computationally demanding if the number of objectives is large [36, 39]. This is the reason why some existing approaches for multi-objective HEM optimization are not suitable for many-objective problems. For instance, the epsilon-constraint method requires the solution of many single-objective problems to generate the set of Pareto solutions [26]. In addition, this approach confers, a priori, the same importance to all the objective functions, which is not a reasonable assumption as commented before.

In this section, we propose a novel many-objective optimization paradigm suitable for HEM programs. The new proposal only requires the solution of $N_p + 1$ single objective problems, and allows to rank the objective functions thus one of them is considered more important than the others. The developed approach is based on the lexicographic optimization and scalarizing functions, which are briefly explained below, referring the reader to the vast existing literature for further information (e.g. see [47]).

5.1 - Lexicographic optimization

The Lexicographic optimization is an '*a priori'* method that allows to solve contradictory multi-objective problems ranking the different objectives according to their given importance. Let us suppose a multi-objective problem with N_p objectives, i.e. $\boldsymbol{f} = \left\{f_1, \dots, f_{N_p}\right\}$; in which, without loss of generality, the objectives are correlativity ordered according to their importance. Thus, the lexicographic method is carried out by iteratively solving N_p single-objective sub-problems with the form

$$\begin{aligned} &\min_{\boldsymbol{x}} f_i \\ &\text{s.t.}\, f_j = \underline{f_i};\, j = 1, \dots, N_p - 1 \\ &\boldsymbol{x} \in \Xi \end{aligned} \tag{48}$$

where Ξ is the feasible solution space and $\boldsymbol{x} \in \mathbb{R}^n$ is the vector of decision variables. A major disadvantage of this method is that it tends to favor certain objectives, making the Pareto front converge to a particular region [48]. However, this particular disadvantage is not conflictive in HEM problems where the electricity bill is typically the most important objective.

5.2 - Scalarizing functions

The most conventional and simplest methodology for solving multi-objective problems consists on converting them to single-objective ones by using scalarizing functions. In their most general form, a generic multi-objective problem is converted to the following single-objective one by using a well-defined scalarizing function

$$\begin{aligned}&\min_{\boldsymbol{x}} \psi(\boldsymbol{f})\\&\mathrm{s.t.}\, \boldsymbol{x} \in \Xi\end{aligned} \tag{49}$$

where $\psi: \mathbb{R}^n \mapsto \mathbb{R}$ is a given scalarizing function. The most typical scalarizing function is the weighted sum of objectives [49].

5.3 - Proposed approach

The new proposal assumes that one of the objectives involved in the HEM problem has a clear higher importance, while the other objectives are conferred with similar significance. This assumption is reasonable in HEM programs, in which, as commented, the reduction of the electricity bill is usually the main concern for home users. Therefore, let us classify the objectives into two groups called primary and secondary objectives. Without loss of generality, f_1 will be the primary objective while the others, i.e. $f_2,\ldots,f_{N_p}$; define the set of secondary objectives. With these considerations, the first step of the proposed approach consists on solving the following N_p single-objective sub-problems.

$$\begin{aligned}&\boldsymbol{x}_i^* \rightarrow \arg\min_{\boldsymbol{x}} f_i\,; i = 1,2, \ldots, N_p\\&\mathrm{s.t.}\, \boldsymbol{x} \in \Xi\end{aligned} \tag{50}$$

Solution of (50) for the N_p objectives allow to calculate the utopia and pseudo-Nadir points on the objective-space [26]. The meaning of these points is pictorially represented in Fig. 2, where the objective-solution space for a generic bi-objective optimization problem is depicted. As seen in this figure, the utopia and pseudo-Nadir points for the different objective functions involved in the problem can be calculated by using (51) and (52), respectively.

$$f_i^{\mathrm{U}} = f_i(\boldsymbol{x}_i^*); i = 1,2, \ldots, N_p \tag{51}$$

$$f_i^{\mathrm{SN}} = \max\left(f_i(\boldsymbol{x}_1^*), \dots, f_i(\boldsymbol{x}_j^*), \dots, f_i\left(\boldsymbol{x}_{N_p}^*\right)\right); i = 1,2, \dots, N_p \tag{52}$$

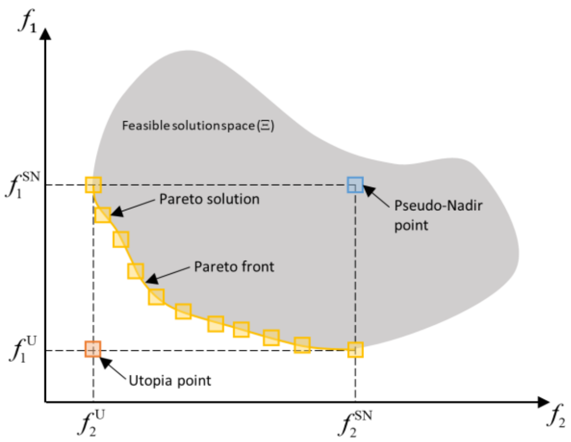

Fig. 2 Location of the utopia and pseudo-Nadir points on a generic bi-objective solution space

By definition, the utopia and pseudo-Nair points suppose upper and lower bounds for each objective function since all the sub-problems in (50) are defined as minimization problems (i.e. $f_i^{\mathrm{U}} = \underline{f_i}, f_i^{\mathrm{SN}} = \overline{f}_i;\ i = 1,2, \dots, N_p$).

By solving (50), the desired value for the primary objective function is naturally obtained as it is equal to its utopia point. It is assumed that remainder objectives should be optimized without degrading this objective, it means, the secondary objectives should be minimized subjected to $f_1(\boldsymbol{x}) = f_1^{\mathrm{U}}$. In practise, it supposes a very tight restriction which notably limits the degree for which remainder objectives could be achieved. In this sense, we introduce a relaxing factor $q \geq 1$, that defines the level by which the users are willing to sacrifice the main objective to enhance the secondary ones. Therefore, whatever the solution of the multi-objective problem calculates, the following constraint must be satisfied.

$$f_1(\boldsymbol{x}) \leq q \cdot f_1^{\mathrm{U}} \tag{53}$$

As commented, the secondary objectives are assumed to have similar importance within the optimization paradigm. In this sense, all of them can be grouped into a single-objective problem by using scalarizing functions. Thereby, the solution of the multi-objective problem by using the proposed approach is achieved by solving the following lexicographic optimization scheme.

$$\begin{aligned}&\min_{\boldsymbol{x}} \psi\left(f_2, \dots, f_{N_p}\right)\\&\text{s.t. } (53)\\&\boldsymbol{x} \in \Xi\end{aligned} \tag{54}$$

For solving (54), any existing scalarizing function could be used. In this paper, we have considered the weighted sum of the normalized objectives because its linearity and simplicity, as follows

$$\psi\left(f_2, \dots, f_{N_p}\right) = \sum_{i=2}^{i=N_p} \left\{w_i \cdot \frac{f_i(\boldsymbol{x}) - f_i^{\mathrm{SN}}}{f_i^{\mathrm{U}} - f_i^{\mathrm{SN}}}\right\} \tag{55}$$

For the sake of summarizing, Fig. 3 shows the flowchart of the proposed approach for many-objective optimization. As seen, our proposal only requires to solve $N_p + 1$ optimization problems. Other approaches, require to solve many optimization problems, for example [26], by which the Pareto front is divided in grid-point sections and any of the grid areas has to be analysed by running an individual optimization problem. This approach may further explore the Pareto front on searching Pareto-optimal solutions, however, as empirically demonstrated in Section 7.3, the quality of the results obtained with the new proposal is not compromised and are totally acceptable in practise. On the other hand, Fig. 4 pictorially illustrates the developed many-objective solution procedure over a generic three-objective solution space. As seen, our proposal finds the point in the Pareto front for which ψ is minimized while the primary objective is kept below an acceptable threshold. The relaxation introduced on the primary objective function allows to further minimize the secondary objectives.

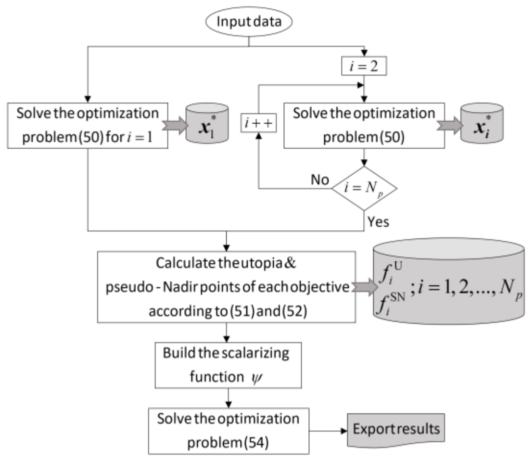

Fig. 3 Flowchart of the developed methodology for many-objective optimization

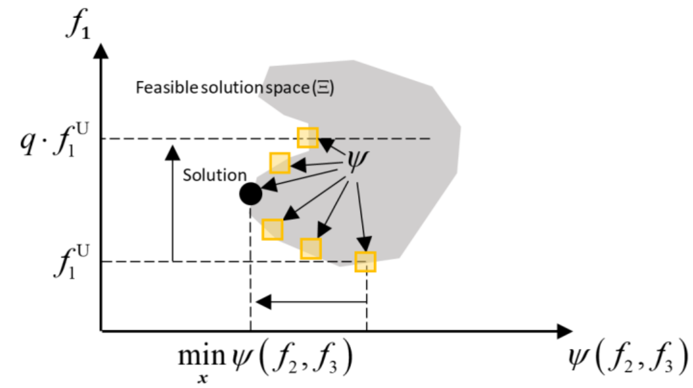

Fig. 4 Illustration of the developed approach for many-objective optimization on the solution space

5.4 - Application of the proposed approach to the HEM problem

The developed many-objective approach described in Section 5.3 is especially suitable for HEM programs. In such problems, the reduction of the electricity bill (f_1) is frequently considered the primary objective function for home tenants, so that they are unwilling to satisfy other objectives if this supposes a notably increment on their monetary expenditures. In this sense, this objective can be defined as the primary target whereas the group of secondary goals encompasses the functions $f_2 - f_6$ described in section 4. Thus, taking the HEM problem described in Section 3 and the functions $f_1 - f_6$ as benchmark, the adaptation of the developed approach for many-objective HEM programs is given by

$$\min_{\boldsymbol{x}} \frac{1}{N_p - 1} \cdot \sum_{i=2}^{i=N_p} \left\{ \frac{f_i(\boldsymbol{x}) - f_i^{\mathrm{SN}}}{f_i^{\mathrm{U}} - f_i^{\mathrm{SN}}} \right\}$$
$$\text{s.t.} (1) - (27), (32), (33), (36) - (42), (44), (45) \tag{56}$$
$$f_1(\boldsymbol{x}) \leq q \cdot f_1^{\mathrm{U}}$$

where $\boldsymbol{x} = \left[\Phi, p_r^{\mathrm{Peak}}, y_{r|t}, z_{r|t}, v_r^k\right]$; $\forall r \in \mathcal{R}, t \in \mathcal{T}, k \in \mathcal{K}^{\mathrm{I}}$. It is worth noting that, for simplicity, all the weights have been taken equal in the scalarizing function in (56), thus all the secondary objectives have the same importance. Nevertheless, they could be freely fixed as needed.

6 - Uncertainties modelling

The HEM problem is subjected to multiple uncertain parameters such as ambient temperature, solar irradiation or non-controllable appliances demand, among others, which should not be ignored at all. In order to properly validate the developed many-objective paradigm, these stochastic parameters are treated via scenarios. This aspect has a direct impact in the computational burden of the developed approach, thus allowing us further analysing its computational tractability. In this sense, the computational burden of the whole optimization algorithm is expected to be proportional to the size of the scenario space. To this end, we propose a simple but effective approach that presents modular structure and can be applied with different optimization techniques.

To generate the scenarios that are involved in the mathematical solution of the HEM program, we assume that all the uncertainties can be day-ahead forecasted with sufficiently accuracy. Then, it is assumed that forecast errors follow a Gaussian distribution with mean equal to the forecasted value. The unpredictable behaviour of the forecast errors can be catch if a sufficiently large number of scenarios is generated according to their probability distribution functions (1,000 scenarios are usually considered adequate [50]). Nevertheless, the large amount of scenarios that are required for capturing the stochastic nature of the errors is difficulty tractable in practise. To reduce the amount of data to be treated one can use clustering techniques [51], in order to only consider the most representative profiles. This way, the set of data generated is grouped into clusters (Ω) within which the elements are as similar as possible and thus can be represented by a single member. Thereby, the scenario set $\mathcal{S}$ is reduced to the representative scenario set $\mathcal{R}$, which is actually used in simulations. In this sense, the procedure described in [42] has been used in this paper, by which the scenarios generated are clustered using the k-medoids method. Intuitively, much less scenarios are in fact considered in simulations since ~10-20 clusters are typically sufficient to reliable represent a set of raw data [10, 44]. As explained in [42], the total number of clusters required can be fixed heuristically by observing some helpful indicators. One salient feature of the k-medoids technique is the possibility of easily calculating the probability of each representative scenario as follows

$$\omega_r = \frac{\text{size}(\Omega_r)}{\text{size}(\mathcal{S})};\ \forall r \in \mathcal{R} \tag{57}$$

It is worth noting that the framework presented in this section for uncertainties modelling is not defined for any stochastic parameter in particular. This feature reveals a modular structure which allows to consider any uncertainty as the problem requires.

7 - Case study

Throughout this Section, various results are presented and discussed to validate and assessing the computational efficiency of the developed approach. The simulations have been performed for a 24 h time horizon, taking a time step of 30 min and considering the home system described in Section 2, which could be assumed as a benchmark home layout [10, 25, 31]. The value of the factor q has been taken equal to 1.05, which means that home users would be willing to increment the electricity bill by 5% to satisfy other secondary objectives. The developed HEM program based on MILP formulation has been coded on Matlab R2019a and solved with Gurobi [52].

7.1 - Input data

In simulations, it is considered that the maximum power that can be purchased from the utility grid is 5 kW. A typical Time-of-use energy price has been considered [53], which is shown in Fig. 5. Small-scale PV array and BES Li-ion system are considered, whose parameters are tabulated in Tables 1 and 2, respectively. Tables 3-5 collect the data related to the thermostatically controlled appliances, which have been taken from [21, 31]. The parameters of the PEV are reported in Table 6 and corresponds to a Renault Zoe (22 kWh). The data of the controllable appliances is listed in Table 7 [13, 25].

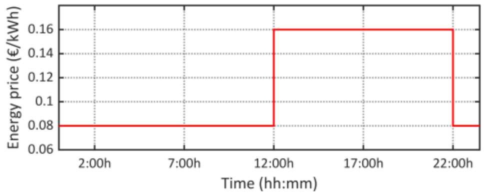

Fig. 5 - Time-of-use tariff used in simulations

Table 1 - Data of the PV array

Parameter	Value
Peak power	0.5 kWp
Efficiency	0.167

Table 2 - Data of the BES system

Parameter	Value
Capacity	5 kWh
Rated power	2 kW
Efficiency	0.98
Depth of discharge	0.70

Table 3 - Thermal data of the building

Parameter	Value
Equivalent thermal resistance	$3.20 \cdot 10^{-6}$ (J/ºC)
Heat capacity of the air	1.01 (kJ/(kg · ºC))
Mass of air	1,778.40 kg

Table 4 - Data of the HVAC system

Parameter	Value
Rated power	2 kW
Coeff. of performance	1.20
Temperature set-point	23 ºC
Temperature dead-band	0.50 ºC

Table 5 - Data of the EWH

Parameter	Value	Parameter	Value
Rated power	2.10 kW	Efficiency	0.90
Heat capacity of the water	1.52 (ºC/kW)	Set-point	45 ºC
Equivalent thermal resistance	863.40 (ºC/kWh)	Max. Temperature	60 ºC
Capacity	50 gal	Cold water temperature	10 ºC

Table 6 - Data of the PEV

Parameter	Value
Capacity	22 kWh
Rated power	3 kW
Efficiency	0.98
Depth of discharge	0.80
Time window	0:00-6:30 h

Table 7 - Data of the controllable appliances

Appliance	Nominal power	Time window	δ	Type
Washing machine	3 kW	7:30-11:00 h	3	Non-interruptible
Dishwasher	2.50 kW	7:00-16:00 h	4	Interruptible
Spin dryer	2.50 kW	12:00-17:00 h	2	Interruptible

Five source of uncertainties have been considered, i.e. solar irradiation, ambient temperature, hot water consumption, non-controllable appliances demand and initial state-of-charge of the PEV. Forecast values for the solar irradiation and ambient temperature have been taken for a typical day at Madrid (Spain) throughout the year 2016 [54]. For the hot water consumption, the demand pattern described in [55] has been considered as forecast profile. The non-controllable appliances demand has been generated according the metering data available in [56], whereas the predicted initial state of charge of the PEV has been taken equal to 50% of its nominal capacity [25]. These profiles have been converted to per unit values and Gaussian distributions with standard deviation 0.1 has been used for generating 1,000 scenarios. For the initial state-of-charge of the PEV, following the methodology described in [25], 1,000 scenarios have been generated using a truncated Gaussian distribution ranging from 0.3 to 0.95 and standard deviation equal to 0.25. The constructed scenarios have been reduced to 18 representative profiles using the k-medoids technique and the procedure described in [42]. Fig. 6 plots the different scenarios considered in simulations for the weather and demand uncertainties.

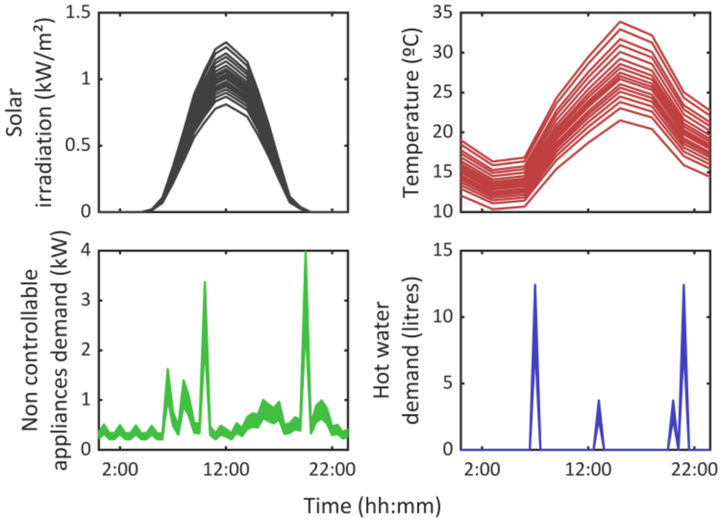

Fig. 6 The 18 scenarios considered for modelling uncertainties in simulations

7.2 - Results

Fig. 7 shows the value of the objective functions $f_1 - f_6$ when the optimization problem (50) is individually carried out for each objective function (i.e. with $i = 1,2, \dots ,6$). As expected, each objective is minimised when itself is taking as target in the scheme (50), whereas the other functions take different values. These results show the contradictory nature of the different objectives described in sections 3 and 4. For example, it is clear that the thermal comfort and the energy cost are contradictory targets since, as seen in Fig. 5, the maximization of the former is achieved at the expense of increasing the latter, and vice versa.

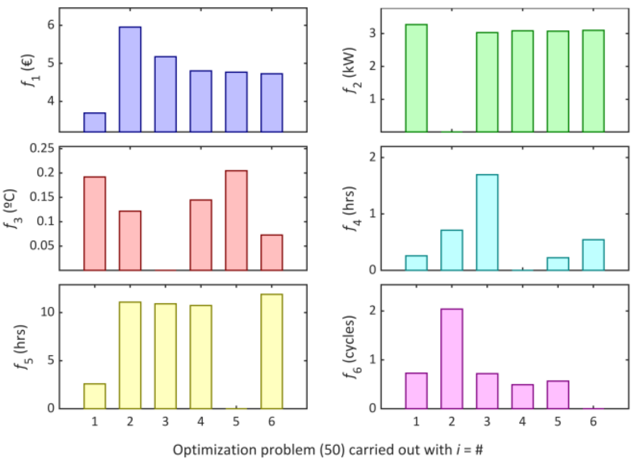

Fig. 7 The value of each objective function running the optimization problem (50) taking the different functions as objectives individually

Contradictory nature of the different objective functions is more clearly illustrated in Fig. 8, where the scheduling results are compared for each running of the optimization problem (50) taking $f_1 - f_6$ as objective functions, individually. As observed, the different assets are scheduled thus each objective function is minimized. For example, when the PAR is aimed to be reduced at minimum, the home system purchases excessive power from the grid in order to flatten its load curve, however, this objective is reached at the expense of reducing the exploitation of the PV array, incrementing the electricity bill notably. This evidences the necessity of considering the HEM problem as a multi-objective paradigm rather than a single-objective problem. On the other hand, when f_4 is taken as objective, the non-interruptible appliances (washing machine) are scheduled at the beginning of their time window (7:30 h). Similarly, when f_5 is taken as objective, the interruptible appliances begin their duty cycles at the beginning of their time windows and, in addition, they work as non-interruptible appliances in order to reduce the waiting time to the minimum. An extreme case is observed when f_6 is minimized since, in this case, the minimum number of charging-discharging cycles is achieved when the BES is not exploited at all. The impact of the thermal comfort is more understandably by observing Fig. 9, where the indoor temperature is compared for the cases in which f_1 and

f_3 are individually compared. As seen in this figure, when the thermal comfort is maximized the HVAC is operated thus keep the room temperature at the specified set-point through the considered time horizon. Contrarily, the indoor temperature varies from the set-point to admissible limits in order to reduce the electricity bill in the case of f_1 is minimized, which is reached by reducing the energy consumption of the HVAC system.

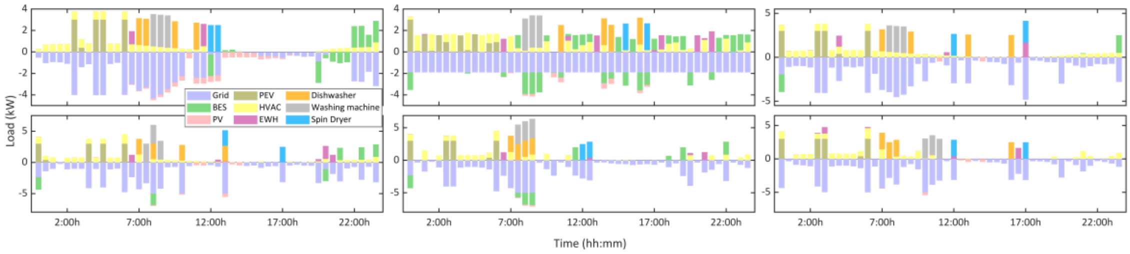

Fig. 8 Scheduling result after running the optimization problem (50) optimizing f_1 (upper left), f_2 (upper middle), f_3 (upper right), f_4 (bottom left), f_5 (bottom middle) and f_6 (bottom right). In this figure, negative powers indicate ‘to home’ flow direction (generation)

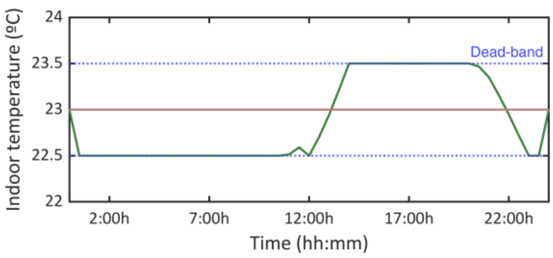

Fig. 9 Indoor temperature after running the problem (50) optimizing f_1 (green line) and f_3 (red line)

Table 8 reports the utopia and pseudo-Nadir points of each objective function. Since f_1 is considered the most important objective function, its utopia point has been taken as reference to perform the lexicographic scheme (56). Since it has been assumed that the home inhabitants are willing to let the electricity bill increments by 5% in order to satisfy other secondary objectives (i.e. $q = 1.05$), $g_1 = 3.88$ € supposes an upper bound for the constraint (53). With these assumptions the optimization problem (56) has been carried out and the results are also reported in Table 8. As seen, the optimization problem (56) achieves a compromise solution of all secondary objectives which are located between their respective utopia and pseudo-Nadir points. These objectives are, however, achieved by incrementing the electricity bill to their maximum allowed value. The scheduling result obtained after solving the problem (56) is plotted in Fig. 10.

Table 8 - The utopia, pseudo-Nadir and Many-objective values of the different objective functions

Objective	Utopia	Pseudo-Nadir	Many-objective result
f_1 (€)	3.69	5.95	3.88
f_2 (kW)	0.01	3.28	1.01
f_3 (ºC)	0	10.02	0.02
f_4 (hrs)	0	0.90	0
f_5 (hrs)	0	11.90	2.06
f_6 (cycles)	0	2.04	1.09

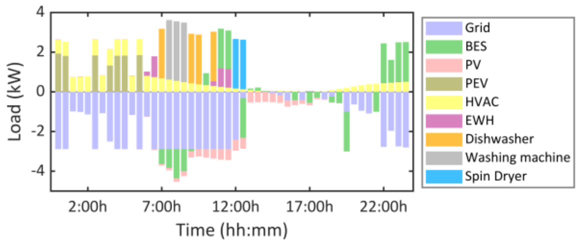

Fig. 10 Scheduling result obtained after running the lexicographic problem (56). In this figure, negative powers indicate 'to home' flow direction (generation)

7.3 - Comparison with the ϵ-constraint method

This section is devoted on comparing the developed many-objective approach with the ϵ-constraint method developed in [26, 57]. In this sense, we consider the same value of q used in previous simulations and the same weight is given to all secondary objectives. Table 9 reports the value of the different objective functions calculated by the two approaches; as seen, both methods achieved similar solutions. The marginal differences among the results reported in Table 9 demonstrates that the developed approach and the ϵ-constraint technique were able to explore the same area on the Pareto front and therefore calculated the same result in practical terms. This means that both approaches are in fact effective and accurate since, if any of them were focused on a different zone of the Pareto front, more notably differences should be observed. This is clearly illustrated in Fig. 2 and 4. As seen in these figures, small differences in the objective functions are only possible when the same area of the Pareto front is explored, on the contrary, larger differences should be observed which is not certainly the case reported in Table 9. Therefore, one can conclude that both the developed approach and the ϵ-constraint technique calculated in fact the same solution, and the small differences encountered were due to the mathematical procedure rather than accuracy issues.

In addition, it is clear that solution calculated by both methodologies is the same in practise and therefore the impact of the small differences observed can be considered negligible. Analysing in particular the function f_3, this difference is 0.17 ºC. It means that, regarding the HVAC, the scheduling result calculated by the ϵ-constraint approach accumulates an error of 0.17 ºC higher than the same result calculated by the developed approach. If this error is assumed constant throughout the time horizon, the difference in the room temperature between the two compared techniques is lower than 0.004 ºC each time step, which is certainly insignificant and not perceptible by home inhabitants.

Table 9 - Results obtained with the ϵ-constraint method [26, 57] and the developed solution method

Objective	**Developed**	**ϵ-constraint**
f_1 (€)	3.88	3.87
f_2 (kW)	1.01	1.12
f_3 (ºC)	0.02	0.19
f_4 (hrs)	0	0
f_5 (hrs)	2.06	2.00
f_6 (cycles)	1.09	0.93

One of the presumably salient features of the developed approach is its low computational burden. In this regard, we run our proposal and the ε-constraint method on an Intel® Core™ i7-8750H 2.20 GHz 16.00 GB RAM personal laptop. Fig. 11 compares the computational cost of both approaches to solve the HEM problem with different number of objective functions. In order to obtained reliable results, the reported times have been calculated as the average time of 100 simulations to minimize the impact of background computational activities [58]. As seen, computational time exponentially grows with the number of objective functions involved. However, the ϵ-constraint technique turned out to be more time consuming that the developed approach. These results are coherent with the conclusions drawn in [39], were it is pointed out the inefficiency of the ϵ-constraint technique in many-objective problems.

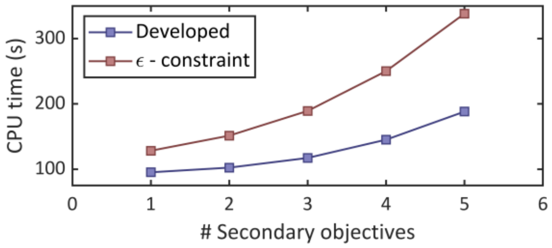

Fig. 11 Comparison of computational time of the developed approach and the ϵ-constraint methods for different number of secondary objectives

Lastly, we compare the impact of the uncertainties modelling in the computational performance of both solution procedures. In this sense, the total number of scenarios considered presumably affects the total time consumed by both approaches. Thus, the higher the number of scenarios, the more time consuming the optimization problem is. This statement is confirmed by the results reported in Fig. 12, where the time consumption of both compared methodologies is plotted for different sizes of the representative scenario space. As seen in this figure, the size of the scenario space affects much more notably to the ϵ-constraint technique, whose computational time significantly grows with the total number of scenarios considered.

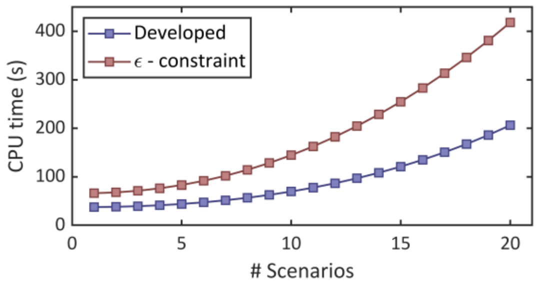

Fig. 12 Comparison of computational time of the developed approach and the ϵ-constraint methods for different number of scenarios considered for stochastic programming

8 - Conclusions

A novel many-objective optimization solution procedure especially suitable for Home Energy Management systems has been presented in this paper. The new proposal is based on lexicographic optimization and scalarizing functions, and allow to select one of the objectives as the most important one whereas the others can be classified as secondary targets. This feature is especially relevant for Home Energy Management tools in which the minimization of the energy cost is conventionally perceived as the most important goal while other targets such as maximization of the thermal comfort frequently receive less importance. Other salient features of the developed methodology are its modularity and ability to achieve the global optimum because its Mixed Integer Linear Programming formulation. A simple modular strategy for incorporating uncertainties has been also presented.

The developed approach has been validated on a standard home layout. The results have evidenced the ability of the new proposal to reach a compromise solution among all the secondary objectives without increasing the electricity bill. The new proposal has been compared with the ϵ-constraint method, proving that both techniques achieve similar results. However, the developed framework has turned out to be much more efficient, showing that the novel methodology is computationally light and can be efficiently managed by average computers and off-the-self solvers.

Future works will be devoted on applying the developed approach to other many-objective problems such as Microgrid expansion planning.

Acknowledgments

The icons used in this manuscript were developed by Freepik and Smashicons from www.flaticon.com

References

[1] U. S. Department of Energy. The Smart Grid: an Introduction; 2008. Available at: https://www.energy.gov/oe/downloads/smart-grid-introduction-0; [Accessed May 3, 2021].

[2] Y. Xue, X. Yu. Beyond smart grid-cyber-physical-social system in energy future [point of view]. *Proceedings of the IEEE* 2017; 15(12): 2290-2. 10.1109/JPROC.2017.2768698.

[3] L. Tao, Y. Gao. Real-time pricing for smart grid with distributed energy and storage: A noncooperative game method considering spatially and temporally coupled constraints. *International Journal of Electrical Power & Energy Systems* 2020; 115: 105487. 10.1016/j.ijepes.2019.105487.

[4] J. Jo, J. Park. Demand-Side Management With Shared Energy Storage System in Smart Grid. *IEEE Transactions on Smart Grid* 2020; 11(5): 4466-76. 10.1109/TSG.2020.2980318.

[5] C. Lu, B. Shi, X. Wu, H. Sun. Advancing China's Smart Grid: Phasor Measurement Units in a Wide-Area Management System. *IEEE Power & Energy Magazine* 2015; 13(5): 60-71. 10.1109/MPE.2015.2432372.
[6] N. Gudi, L. Wang, V. Devabhaktuni. A demand side management based simulation platform incorporating heuristic optimization for management of household appliances. *International Journal of Electrical Power & Energy Systems* 2012; 43(1): 185-93. 10.1016/j.ijepes.2012.05.023.
[7] M. Rastegar, M. Fotuhi-Firuzabad, H. Zareipour. Home energy management incorporating operational priority of appliances. *International Journal of Electrical Power & Energy Systems* 2016; 74: 286-92. 10.1016/j.ijepes.2015.07.035.
[8] J. S. Vardakas, N. Zorba, C. V. Verikoukis. A Survey on Demand Response Programs in Smart Grids: Pricing Methods and Optimization Algorithms. *IEEE Communications Surveys & Tutorials* 2015; 17(1): 152-78. 10.1109/COMST.2014.2341586.
[9] K. Ma, T. Yao, J. Yang, X. Guan. Residential power scheduling for demand response in smart grid. *International Journal of Electrical Power & Energy Systems* 2016; 78: 320-5. 10.1016/j.ijepes.2015.11.099.
[10] M. Tostado-Véliz, S. Mouassa, F. Jurado. A MILP framework for electricity tariff-choosing decision process in smart homes considering 'Happy Hours' tariffs. *International Journal of Electrical Power & Energy Systems* 2021; 131: 107139. 10.1016/j.ijepes.2021.107139.
[11] Y. Huang, H. Tian, L. Wang. Demand response for home energy management system. *International Journal of Electrical Power & Energy Systems* 2015; 73: 448-55. 10.1016/j.ijepes.2015.05.032.
[12] C. O. Adika, L. Wang. Smart charging and appliance scheduling approaches to demand side management. *International Journal of Electrical Power & Energy Systems* 2014; 57: 232-40. 10.1016/j.ijepes.2013.12.004.
[13] A. Shewale, A. Mokhade, N. Funde, N. D. Bokde. An Overview of Demand Response in Smart Grid and Optimization Techniques for Efficient Residential Appliance Scheduling Problem. *Energies* 2020; 13(16): 4266. 10.3390/en13164266.
[14] Y. Zhang, P. Zeng, S. Li, C. Zhang, H. Li. A Novel Multiobjective Optimization Algorithm for Home Energy Management System in Smart Grid. *Mathematical Problems in Engineering* 2015; 2015: 807527. 10.1155/2015/807527.
[15] Y. Lin, M. Tsai. An Advanced Home Energy Management System Facilitated by Nonintrusive Load Monitoring With Automated Multiobjective Power Scheduling. *IEEE Transactions on Smart Grid* 2015; 6(4): 1839-51. 10.1109/TSG.2015.2388492.
[16] A. Anvari-Moghaddam, H. Monsef, A. Rahimi-Kian. Optimal Smart Home Energy Management Considering Energy Saving and a Comfortable Lifestyle. *IEEE Transactions on Smart Grid* 2015; 6(1): 324-32. 10.1109/TSG.2014.2349352.
[17] L. Geng, Y. Wei, Z. Lu, Y. Yang. A novel model for home energy management system based on Internet of Things. In: *2016 IEEE International Conference on Power and Renewable Energy (ICPRE)*; Shanghai, China, 2016: 474-80. 10.1109/ICPRE.2016.7871256.
[18] S. Rahim, et al. Exploiting heuristic algorithms to efficiently utilize energy management controllers with renewable energy sources. *Energy & Buildings* 2016; 129: 452-70. 10.1016/j.enbuild.2016.08.008.
[19] C. Guzman, A. Cardenas, K. Agbossou. Evaluation of meta-heuristic optimization methods for home energy management applications. In: *2017 IEEE 26th International Symposium on Industrial Electronics (ISIE)*; Edinburgh, UK, 2017: 1501-6. 10.1109/ISIE.2017.8001468.
[20] X. Jin, K. Baker, D. Christensen, S. Isley. Foresee: A user-centric home energy management system for energy efficiency and demand response. *Applied Energy* 2017; 205: 1583-95. 10.1016/j.apenergy.2017.08.166.
[21] M. Shafie-Khah, P. Siano. A Stochastic Home Energy Management System Considering Satisfaction Cost and Response Fatigue. *IEEE Transactions on Industrial Informatics* 2018; 14(2): 629-38. 10.1109/TII.2017.2728803.
[22] J. M. Veras, et al. A Multi-Objective Demand Response Optimization Model for Scheduling Loads in a Home Energy Management System. *Sensors* 2018; 18(10): 3207. 10.3390/s18103207.
[23] B. Hussain, N. Javaid, Q. U. Hasan, S. Javaid, A. Khan, S. A. Malik. An Inventive Method for Eco-Efficient Operation of Home Energy Management Systems. *Energies* 2018; 11(11): 3091. 10.3390/en11113091.

[24] J. Zupančič, B. Filipič, M. Gams. Genetic-programming-based multi-objective optimization of strategies for home energy-management systems. *Energy* 2020; 203: 117769. 10.1016/j.energy.2020.117769.

[25] M. S. Javadi, M. Gough, M. Lotfi, A. E. Nezhad, S. F. Santos, J. P. S. Catalão. Optimal self-scheduling of home energy management system in the presence of photovoltaic power generation and batteries. *Energy* 2020; 210: 118568. 10.1016/j.energy.2020.118568.

[26] M. S. Javadi, et al. Self-scheduling model for home energy management systems considering the end-users discomfort index within price-based demand response programs. *Sustainable Cities & Society* 2021; 68: 102792. 10.1016/j.scs.2021.102792.

[27] X. Wang, X. Mao, H. Khodaei. A multi-objective home energy management system based on internet of things and optimization algorithms. *Journal of Building Engineering* 2021; 33: 101603. 10.1016/j.jobe.2020.101603.

[28] B. V. Rao, F. Kupzog, M. Kozek. Phase Balancing Home Energy Management System Using Model Predictive Control. *Energies* 2018; 11(12): 3323. 10.3390/en11123323.

[29] A. Amer, K. Shaban, A. Gaouda, A. Massoud. Home Energy Management System Embedded with a Multi-Objective Demand Response Optimization Model to Benefit Customers and Operators. *Energies* 2021; 14(2): 257. 10.3390/en14020257.

[30] M. Alilou, B. Tousi, H. Shayeghi. Home energy management in a residential smart micro grid under stochastic penetration of solar panels and electric vehicles. *Solar Energy* 2020; 212: 6-18. 10.1016/j.solener.2020.10.063.

[31] N. G. Paterakis, O. Erdinç, A. G. Bakirtzis, J. P. S. Catalão. Optimal Household Appliances Scheduling Under Day-Ahead Pricing and Load-Shaping Demand Response Strategies. *IEEE Transactions on Industrial Informatics* 2015; 11(6): 1509-19. 10.1109/TII.2015.2438534.

[32] T. Sattarpour, D. Nazarpour, S. Golshannavaz. A multi-objective HEM strategy for smart home energy scheduling: A collaborative approach to support microgrid operation. *Sustainable Cities & Society* 2018; 37: 26-33. 10.1016/j.scs.2017.09.037.

[33] B. Lokeshgupta, S. Sivasubramani. Cooperative game theory approach for multi-objective home energy management with renewable energy integration. *IET Smart Grid* 2019; 2(1): 34-41. iet-stg.2018.0094.

[34] Q. Lu, Z. Zhang, S. Lü. Home energy management in smart households: Optimal appliance scheduling model with photovoltaic energy storage system. *Energy Reports* 2020; 6: 2450-62. 10.1016/j.egyr.2020.09.001.

[35] S. Chand, M. Wagner. Evolutionary many-objective optimization: A quick-start guide. *Surveys in Operations Research and Management Science* 2015; 20(2): 35-42. 10.1016/j.sorms.2015.08.001.

[36] T. P. Runarsson, et al. Paralell Problem Solving from Nature. In: *Lecture Notes in Computer Science*; G. Goos, J. Hartmanis, J. van Leeuwen (Eds.). Springer-Verlag, Berlin-Heideberg, 2006.

[37] G. Hernández-Rodríguez. Multiobjective optimization of natural gas transportation networks. PhD Thesis 2011; Institut National Polytechnique de Toulouse. Available at: https://oatao.univ-toulouse.fr/7129/1/hernandez_rodriguez.pdf; [Accessed May 4, 2021].

[38] M. Tostado-Véliz, R. S. León Japa, F. Jurado. Optimal Electrification of Off-grid Smart Homes Considering Flexible Demand and Vehicle-to-Home Capabilities. *Applied Energy* 2021; 298: 117184. 10.1016/j.apenergy.2021.117184.

[39] W. Zhang, M. Reimann. A simple augmented ϵ-constraint method for multi-objective mathematical integer programming problems. *European Journal of Operational Research* 2014; 234(1): 15-24. https://doi.org/10.1016/j.ejor.2013.09.001.

[40] M. Javadi, et al. A Multi-Objective Model for Home Energy Management System Self-Scheduling using the Epsilon-Constraint Method. In: *2020 IEEE 14th International Conference on Compatibility, Power Electronics and Power Engineering (CPE-POWERENG)*, Setubal, Portugal, 2020: 175-80. 10.1109/CPE-POWERENG48600.2020.9161526.

[41] S. A. Mansouri, et al. Energy management in microgrids including smart homes: A multi-objective approach. *Sustainable Cities & Society* 2021; 69: 102852. 10.1016/j.scs.2021.102852.

[42] M. Tostado-Véliz, D. Icaza-Álvarez, F. Jurado. A novel methodology for optimal sizing photovoltaic-battery systems in smart homes considering grid outages and demand response. *Renewable Energy* 2021; 170: 884-96. 10.1016/j.renene.2021.02.006.

[43] M. Tostado-Véliz, P. Arévalo, F. Jurado. A comprehensive electrical-gas-hydrogen Microgrid model for energy management applications. *Energy Conversion & Management* 2021; 228: 113726. 10.1016/j.enconman.2020.113726.
[44] P. Arévalo, M. Tostado-Véliz, F. Jurado. A novel methodology for comprehensive planning of battery storage systems. *Journal of Energy Storage* 2021; 37: 102456. 10.1016/j.est.2021.102456.
[45] S. Negarestani, M. Fotuhi-Firuzabad, M. Rastegar, A. Rajabi-Ghahnavieh. Optimal Sizing of Storage System in a Fast Charging Station for Plug-in Hybrid Electric Vehicles. *IEEE Transactions on Transportation Electrification* 2016; 2(4): 443-53. 10.1109/TTE.2016.2559165.
[46] M. Javadi, et al. Optimal Operation of Home Energy Management Systems in the Presence of the Inverter-based Heating, Ventilation and Air Conditioning System. In: *2020 IEEE International Conference on Environment and Electrical Engineering and 2020 IEEE Industrial and Commercial Power Systems Europe (EEEIC / I&CPS Europe)*, Madrid, Spain, 2020: 1-6. 10.1109/EEEIC/ICPSEurope49358.2020.9160629.
[47] Y. Collette, P. Siarry. Multiobjective Optimization. In: *Decision Engineering*; A. Doyle (Ed.). Springer-Verlag, Berlin-Heideberg, 2004.
[48] C. Azzaro-Pantel. Hydrogen Supply Chains (ch. 10). Academic Press, Cambridge, MA, 2018. 10.1016/C2016-0-00605-8.
[49] T. Chugh. Scalarizing Functions in Bayesian Multiobjective Optimization. In: *2020 IEEE Congress on Evolutionary Computation (CEC)*, Glasgow, UK, 2020: 1-8. 10.1109/CEC48606.2020.9185706.
[50] H. Rashidizadeh-Kermani, M. Vahedipour-Dahraie, A. Anvari-Moghaddam, J. M. Guerrero. A stochastic bi-level decision-making framework for a load- serving entity in day-ahead and balancing markets. *International Transactions on Electrical Energy Systems* 2019; 29(11): e12109. 10.1002/2050-7038.12109.
[51] H. Rashidizadeh-Kermani, M. Vahedipour-Dahraie, M. Shafie-khah, J. P. S. Catalão. A bi-level risk-constrained offering strategy of a wind power producer considering demand side resources. *International Journal of Electrical Power & Energy Systems* 2019; 104: 562-74. 10.1016/j.ijepes.2018.07.038.
[52] Gurobi Optimizer Reference Manual. Available at: https://www.gurobi.com/wp-content/plugins/hd_documentations/documentation/9.1/refman.pdf; [Accessed May 7, 2021].
[53] Endesa - Electricity rates catalog. Available at: https://www.endesa.com/en/catalog [Accessed May 7, 2021].
[54] European Comission. Photovoltaic Geographical Information System. Available at: https://re.jrc.ec.europa.eu/pvg_tools/en/tools.html [Accessed May 7, 2021].
[55] A. Rosin, et al. Performance and feasibility analysis of electricity price based control models for thermal storages in households. Sustainable Cities & Society 2017; 32: 366-74. 10.1016/j.scs.2017.04.008.
[56] T. Singh. Smart Home Dataset with weather Information. Available at: https://www.kaggle.com/taranvee/smart-home-dataset-with-weather-information [Accessed May 7, 2021].
[57] A. E. Nezhad, A. Ahmadi, M. S. Javadi, M. Janghorbani. Multi-objective decision-making framework for an electricity retailer in energy markets using lexicographic optimization and augmented epsilon-constraint. *International Transactions on Electrical Energy Systems* 2015; 25(12): 3660-80. https://doi.org/10.1002/etep.2059.
[58] M. Tostado-Véliz, S. Kamel, F. Jurado. An efficient power-flow approach based on Heun and King-Werner's methods for solving both well and ill-conditioned cases. *International Journal of Electrical Power & Energy Systems* 2020; 119: 105869. 10.1016/j.ijepes.2020.105869.